Exposure to Extremely Low-Frequency Electromagnetic Fields Modulates Na$^+$ Currents in Rat Cerebellar Granule Cells through Increase of AA/PGE$_2$ and EP Receptor-Mediated cAMP/PKA Pathway

Yan-Lin He[9], Dong-Dong Liu[9], Yan-Jia Fang, Xiao-Qin Zhan, Jin-Jing Yao, Yan-Ai Mei*

Institutes of Brain Science, School of Life Sciences and State Key Laboratory of Medical Neurobiology, Fudan University, Shanghai, China

Abstract

Although the modulation of Ca^{2+} channel activity by extremely low-frequency electromagnetic fields (ELF-EMF) has been studied previously, few reports have addressed the effects of such fields on the activity of voltage-activated Na$^+$ channels (Na$_v$). Here, we investigated the effects of ELF-EMF on Na$_v$ activity in rat cerebellar granule cells (GCs). Our results reveal that exposing cerebellar GCs to ELF-EMF for 10–60 min significantly increased Na$_v$ currents (I_{Na}) by 30–125% in a time- and intensity-dependent manner. The Na$_v$ channel steady-state activation curve, but not the steady-state inactivation curve, was significantly shifted (by 5.2 mV) towards hyperpolarization by ELF-EMF stimulation. This phenomenon is similar to the effect of intracellular application of arachidonic acid (AA) and prostaglandin E$_2$ (PGE$_2$) on I_{Na} in cerebellar GCs. Increases in intracellular AA, PGE$_2$ and phosphorylated PKA levels in cerebellar GCs were observed following ELF-EMF exposure. Western blottings indicated that the Na$_V$ 1.2 protein on the cerebellar GCs membrane was increased, the total expression levels of Na$_V$ 1.2 protein were not affected after exposure to ELF-EMF. Cyclooxygenase inhibitors and PGE$_2$ receptor (EP) antagonists were able to eliminate this ELF-EMF-induced increase in phosphorylated PKA and I_{Na}. In addition, ELF-EMF exposure significantly enhanced the activity of PLA$_2$ in cerebellar GCs but did not affect COX-1 or COX-2 activity. Together, these data demonstrate for the first time that neuronal I_{Na} is significantly increased by ELF-EMF exposure *via* a cPLA2→AA→PGE$_2$→EP receptors→PKA signaling pathway.

Competing Interests: The authors have declared that no competing interests exist.

* E-mail: yamei@fudan.edu.cn

Introduction

A number of studies have noted that exposure to extremely low-frequency electromagnetic fields (ELF-EMF) alter animal behaviors and modulate biological effects, including changes in gene expression, regulation of cell survival and promotion of cell differentiation [1–3]. In addition, exposure to ELF-EMF induces changes in cerebral blood flow in old Alzheimer's mice. Enzyme activity in the cytosol or at the membrane and subsequent alternations in intracellular signaling are found in lymphoma B cells and Chinese hamster lung (CHL) cells upon exposure to ELF-EMF [4–6]. ELF-EMF can also modify the biophysical properties of cell membranes, such as changes in the membrane permeability of carbonic anhydrase [7], stimulation of the activity of Ca^{2+}-activated potassium channels via increases in Ca^{2+} concentration [3,8] and increased the expression level of Ca^{2+} channel protein [9]. However, very few studies have investigated the effects of EMF on sodium channels, in particular, the voltage-gated sodium (Na$_v$) channels which are highly expressed in neurons.

Voltage-gated sodium channels (Na$_V$) are one of the primary classes of ion channels responsible for driving neuronal excitability in both the central and peripheral nervous system. Na$_V$ are clinically important because they play an important role in the generation of neuronal activity and alterations in Na$_V$ are key factors in a number of pathologies [10]. Recent studies have revealed that Na$_V$ channels participate in the rising phase of the neuronal action potential and contribute to many cellular functions including apoptosis, motility and secretory membrane activity [11–13]. Moreover, the EMF exposure was recently reported to modulate neuronal excitation and neurogenesis, which may be related to Na$_V$ channel activity [8,14,15]. Thus, a thorough investigation of the influence of ELF-EMF on Na$_V$ channels and the corresponding mechanism of action could help to uncover the effects of ELF-EMF-induced biological effects on brain physiology, pathogenesis and neural development.

Cerebellar granule cells (GCs) occupy a key position in the cerebellar–cortical circuitry by forming the input layer of the major cerebellar afferent system. Cerebellar GCs grown in primary culture express tetrodotoxin (TTX)-sensitive Na$_V$ channels which are responsible for action potentials (APs) and for the code relay in the cerebellar circuitry [16,17]. Cerebellar GCs are widely used as a model for neuronal cell development and apoptosis [18–20]. We have previously shown that the I_{Na} densities of cerebellar GCs are modulated by the lipid products ceramide and arachidonic acid (AA). Ceramide reduces the I_{Na} of

cerebellar GCs by increasing calcium release through the ryanodine-sensitive Ca^{2+} receptor [21] while elevation in intracellular AA levels increases the I_{Na} of cerebellar GCs through the PGE$_2$-mediated activation of the cAMP/PKA pathway [22]. The present study was conducted to determine whether exposure to ELF-EMF influences the Na^+ channels of cerebellar GCs and, if so, whether this effect is mediated by changes in ceramide and/or arachidonic acid. The data presented in this report demonstrate that the activity of neuronal Na^+ channels is significantly increased by ELF-EMF stimulation. Notably, the effect of ELF-EMF is mediated by an increase in cPLA$_2$ activity and subsequent changes in intracellular concentration of arachidonic acid (AA) and EP receptor-mediated activation of the cAMP/PKA signaling pathway are involved.

Results

First, we investigated the actions of extremely low frequency electromagnetic fields (ELF-EMF) on the I_{Na} of cerebellar GCs. An I_{Na} was elicited by a depolarization step to -20 mV from the holding potential of -100 mV. When cerebellar GCs were exposed to ELF-EMF (1 mT) for 10 min, the amplitude of the I_{Na} was increased by approximately 51.8% ± 3.8% ($n = 12$, $P<0.05$) compared to cells that were not exposed to ELF-EMF ($n = 8$, Fig. 1A). However, the mean capacitance of recorded cells for the control group (13.05 ± 0.40 pF, $n = 7$) and for the ELF-EMF treatment group (12.45 ± 0.77pF, $n = 6$) showed no significant difference ($P = 0.48$). The similar in capacitance indicated that the increased current density upon ELF-EMF exposure was not due to different in abnormal cell morphology. In addition, the increase in I_{Na} density induced by ELF-EMF exposure was time dependent. When cerebellar GCs were exposed to ELF-EMF for 30 min, 60 min or 90 min, the density of the I_{Na} increased by 67.1% ±4.38% ($n = 8$, $P<0.05$), 125.6% ±8.26% ($n = 16$, $P<0.05$), 102.4% ±4.1% ($n = 9$, $P<0.05$), respectively, compared to controls (Fig. 1B). We also tested the effects of low-density ELF-EMF (0.4 mT) on I_{Na}. The results shown in Fig. 1C indicated that, when cerebellar GCs were exposed to 0.4 mT ELF-EMF, a longer exposure time was needed to induce an increase in I_{Na} density. The density of I_{Na} was only increased by 3.62% ±2.38% ($n = 6$) when cerebellar GCs were exposed to ELF-EMF (0.4 mT) for 6 h. Upon an increase in the length of cell exposure to ELF-EMF (0.4 mT) to 12 h, the I_{Na} density increased by 31.6% ±3.38% ($n = 8$, $P<0.05$, Fig. 1D). Because a previous study indicated that when cells are exposed to ELF-EMF over a long term, their levels of protein expression may be affected [5], which will be difficult to further identify the primary factor involved in the ELF-EMF-induced I_{Na} increase. Thus, we chose to focus on the mechanism by which a relatively short-term exposure to a 1 mT ELF-EMF induces an I_{Na} increase.

Next, we investigated the effects of ELF-EMF on the voltage-gating properties of I_{Na} channels. The activation properties of I_{Na} in cerebellar GCs following exposure to ELF-EMF were studied using the appropriate voltage protocols. I_{Na} were evoked by a 20 ms depolarizing pulse from a holding potential of -100 mV to potentials between -70 and 20 mV, with 5 mV steps 5 s intervals (Fig. 2A). Fig. 2B illustrated a voltage-current curve in which the maximum activation potential was changed from -27.3 ± 0.9 mV to -32.5 ± 2.5 mV when cerebellar GCs were exposed to ELF-EMF for 60 min ($n = 13$ for control and $n = 12$ for ELF-EMF exposure, $P<0.05$). A value for steady-state activation of I_{Na} was then obtained by normalizing the conductance as a function of the command potential; conductance was calculated as $G_{Na} = I_{Na}/(Vm1/2-Vrev)$. The data points were fitted to the Boltzmann

function G_{Na}/G_{Na}-max $= 1/\{1+\exp [(Vm1/2–Vm)/k]\}$. As shown in Fig. 2C, after cerebellar GCs were exposed to ELF-EMF for 60 min, the half-activation potentials changed from -40.93 ± 0.67 mV to -46.87 ± 1.3 5 mV ($n = 10$, $P<0.05$), with slope factors of 3.7 ± 0.1 mV and 4.6 ± 1.0 mV ($n = 10$). These data indicate that ELF-EMF exposure significantly shifts the voltage dependence of the steady-state activation of I_{Na} of cerebellar GCs.

Next, we studied the effects of ELF-EMF exposure on the voltage dependence of the steady-state inactivation of I_{Na} channels. I_{Na} were elicited using 1-s conditioning pre-pulses ranging from -100 to -40 mV in steps of 5 mV prior to a -10 mV test pulse (Fig. 2D). The steady-state inactivation curve was then fitted using the Boltzmann equation $I_{Na}/I_{Namax} = 1/\{1+\exp [(V_m-V_{m1/2})/k]\} +A$. In the 11 cells studied, the $V_{m\ 1/2}$ values were -72.7 ± 0.74 mV ($n = 6$) and -68.2 ± 0.75 mV ($n = 5$) for cells with or without ELF-EMF exposure, respectively (Fig. 2E). These data indicate that the steady-state inactivation curve of I_{Na} in cerebellar GCs did not significantly shift upon exposure to ELF-EMF.

Our previous study showed that elevation in arachidonic acid (AA) concentration increased I_{Na} through prostaglandin E$_2$ (PGE$_2$)-mediated activation of the cAMP/PKA pathway [22]. In the present study, the effect of ELF-EMF exposure on I_{Na} and the I_{Na} steady-state activation curve was similar to the effect of AA on I_{Na}. We therefore tested whether cAMP/PKA activation was involved in the increase in I_{Na} in cerebellar GCs subjected to ELF-EMF exposure. The results in Fig. 3A showed that H-89, a selective PKA antagonist, significantly attenuated the increase in I_{Na} elicited by ELF-EMF exposure. Incubating cerebellar GCs with 10 μM H-89 for 60 minutes decreased the evoked I_{Na} by 42.7% ±4.0% ($n = 9$, $P<0.05$). There was, however, only 12.4% ±6.4% (n = 14) in I_{Na} after exposure to ELF-EMF in the presence of H89. Hence, H89 suppressed the induction of the I_{Na} activity after ELF-EMF exposure. Similarly, administration of 10 μM dibutyryl cAMP (db-cAMP, a embrane-permeable cAMP analog) produced a significant increase of I_{Na} by 47.2 ± 6.6% ($n = 7$, $P<0.05$). Notably, exposure to ELF-EMF did not further potentiate the effect of db-cAMP on I_{Na} (54.8 ± 8.9%, $n = 20$). Hence, these data support our conclusion that cAMP/PKA pathway is involved in the effect of ELF-EMFs on I_{Na}.

In addition, we determined the intracellular levels of phosphorylated PKA (pPKA) by immunoblot assays and found significant increase in phospho-PKA after ELF-EMF exposure. These data indicate that when the cells were exposed to ELF-EMF, the intracellular levels of pPKA were increased by 38.6% ±3.76% ($n = 4$, $P<0.05$), 42.4% ±4.32% ($n = 4$, $P<0.05$),30.4% ±1.5% ($n = 4$, $P<0.05$) and 17.8 ± 2.14% ($n = 4$, $P<0.05$), respectively (Fig. 3C). These data suggest that PKA activation is associated with the ELF-EMF-induced increase in I_{Na} in cerebellar GCs.

Previous study indicated that Na$_V$ activities can be modulated by the cAMP/PKA pathways upon phosphorylation of the α-subunits of Na$_V$ channels [23]. Besides increases in the modification of steady-state activation propriety, exposure to ELF-EMF might also elicit insertion of additional Na$_V$ channels into the membrane, which might then further account for the ELF-EMF-induced up-regulation of I_{Na}. To investigate whether ELF-EMF induced insertion of new Nav channels on the membrane, we first ascertained that Na$_V$ 1.2 α-subunits plays a significant role in Na$_V$ channel of cerebellar GCs as reported previously [17]. As shown in Fig. 4A, the expression of Na$_V$ 1.2 was significantly reduced by siRNA. Similarly, the current amplitude of I_{Na} was also significantly reduced. The current amplitude of I_{Na} recorded from
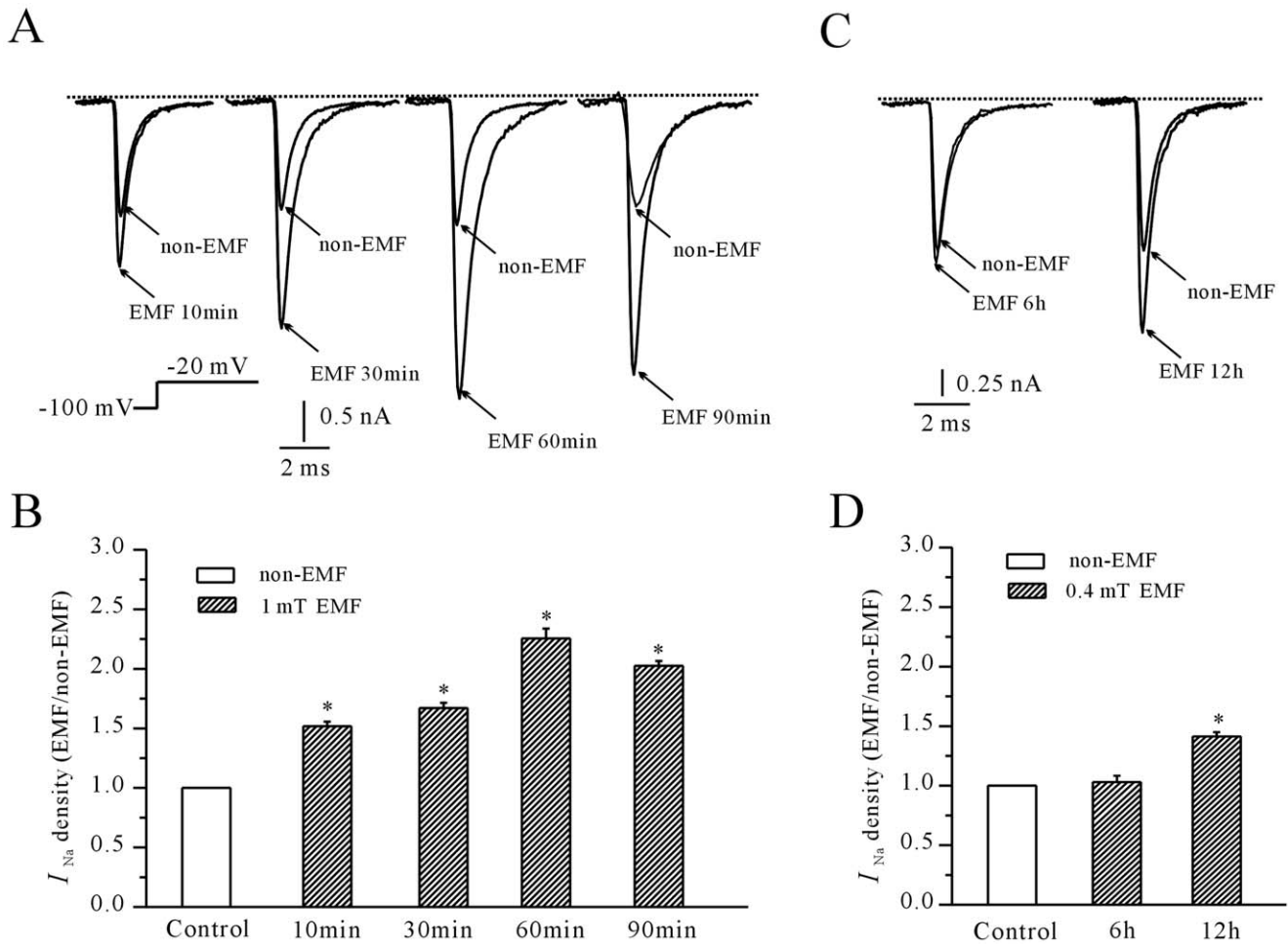
Figure 1. Time-dependent increase in I_{Na} in cerebellar GCs following exposure to ELF-EMF (1 mT or 0.4 mT). Superimposed I_{Na} evoked by a 20 ms depolarizing pulse from a holding potential from −100 to −20 mV. Current traces were obtained from cerebellar GCs exposed to ELF-EMF (1 mT) for lengths of time ranging from 10 min to 90 min. (B) Statistical analysis of the activating effects of ELF-EMF (1 mT) exposure at various times on the density of I_{Na}. The data are reported as the mean ± S.E.M. from 8–16 cells. *, $P<0.05$ compared to control using a one-way ANOVA test. (C) I_{Na} traces obtained from cerebellar cells exposed to ELF-EMF (0.4 mT) for 6 h and 12 h. (D) Statistical analysis of the activating effects of ELF-EMF (0.4 mT) exposure for 6 h and 12 h on the density of I_{Na}. The data are reported as the mean ± S.E.M. from 8–10 cells. *, $P<0.05$ compared to control using Student's t-test.
doi:10.1371/journal.pone.0054376.g001

the control group was −1400.32±162.15 pA ($n=7$), and it was reduced to −207.89±95.55 pA ($n=5$, $P<0.05$) after knocking down the Na$_V$ 1.2 gene (Fig. 4B).

Next, we determined the levels of Na$_V$ 1.2 protein on membrane surface using biotinylation assay. The data obtained from four independent experiments showed that the Na$_V$ 1.2 protein on the cerebellar GCs membrane (Na$_V$ 1.2 M) was increased by 21.8% ±3.3% after exposed to ELF-EMF for 60 min (Fig. 4C). The total expression levels of Na$_V$ 1.2 protein (Na$_V$ 1.2 T), however, was not affected after exposure to ELF-EMF (Fig. 4D). These data indicate that exposure to ELF-EMF activates PKA, which then modulates I_{Na}, in part, by insertion of new Na$_V$ channels into the membrane.

It is well known that the cellular effects of PGE$_2$ are mediated through a family of G-protein-coupled receptors designated EP1, EP2, EP3 and EP4 [24,25]. Of these, EP2 and EP4 are involved in activation of the cAMP/PKA pathway [26]. Our previous study demonstrated that all four types of EP receptors mRNA are found in cerebellar GCs [22]. Because EP2 and EP4 can activate the PKA pathway, we used EP2 and EP4 receptor antagonists

(AH6809 and AH23848, respectively) to investigate whether EP receptors played a role in the activation of PKA after exposure to ELF-EMF. As shown in Fig. 5A and 5B, in the presence of 20 μM AH6809 or 20 μM AH23848, 60 minutes of ELF-EMF exposure only increased I_{Na} by 9.54% ±4.7% ($n=6$) and 5.52±4.71% ($n=5$), respectively. In the absence of the EP receptor antagonists, exposure to ELF-EMF increased I_{Na} to 125.6% ±8.26% ($n=16$, $P<0.05$). Similarly, blocking EP2 and EP4 receptors using AH6809 or AH23848 significantly reduced the ELF-EMF exposure-induced increase in pPKA levels. The results in Fig. 5C showed that in the presence of 20 μM AH6809 or 20 μM AH23848, 60 min of ELF-EMF exposure only increased intracellular levels of pPKA by 7.25% ±1.67% or 6.5% ±2.8% ($n=4$), respectively.

Because EP receptors, which stimulate the cAMP/PKA signaling pathway, are activated by PGE$_2$, we next studied the release of PGE$_2$ from cerebellar GCs following exposure to ELF-EMF using a direct rat PGE$_2$ ELISA kit. As shown in Fig. 6A, the amount of PGE$_2$ released from control cerebellar GCs was 64.36±1.88 pmol. Following exposure to ELF-EMF
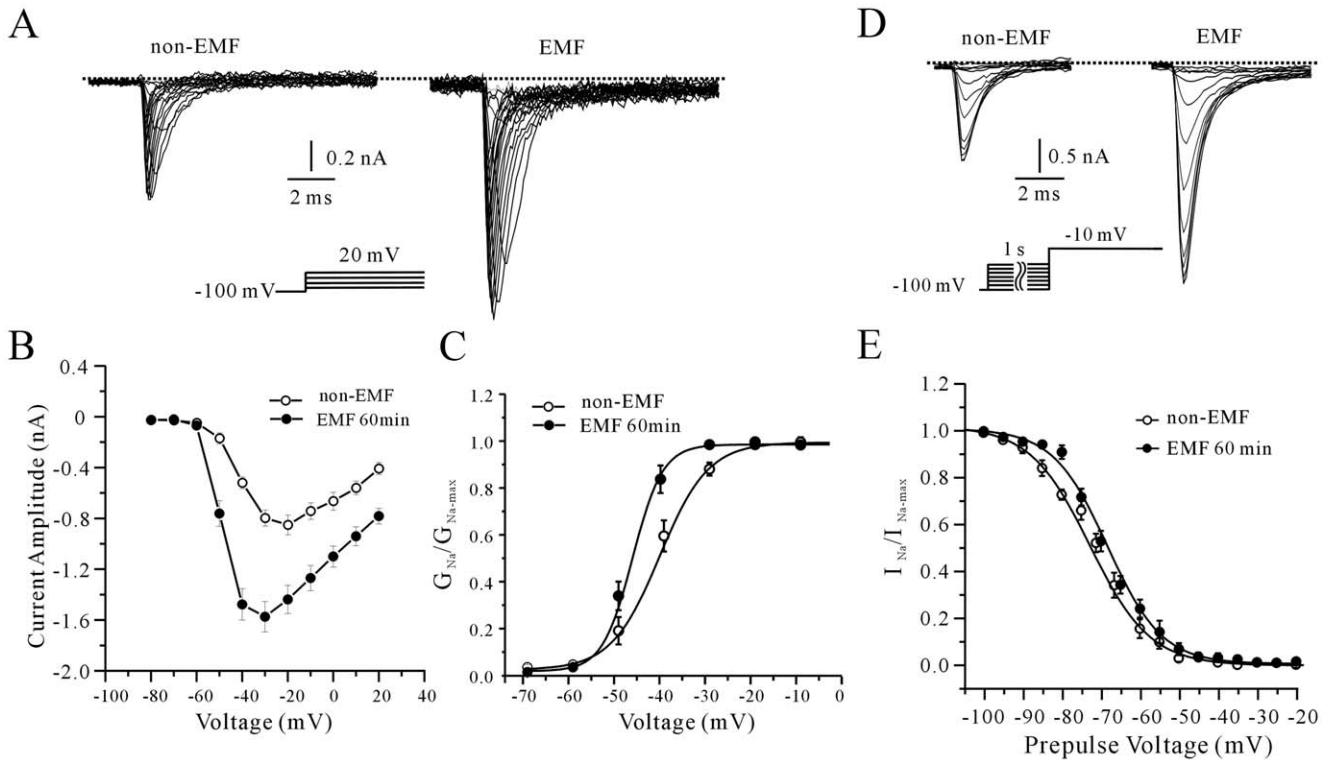
Figure 2. The effects of 1 mT ELF-EMF exposure on the steady-state activation and inactivation of I_{Na}. (A) The effects of 60 minutes of ELF-EMF exposure on the steady-state activation of I_{Na}. The cells were held at −100 mV and depolarized in 5 mV steps from −70 to 20 mV with intervals of 5 s. (B) The voltage-dependent activation curve of I_{Na} in control cells and cells exposed to ELF-EMF. The data are from 13 (control) or 12 (ELF-EMF-exposed) cells and are expressed as means ± SEM. (C) Comparison of the plot of the normalized conductance of I_{Na} as a function of the command potential in control and ELF-EMF-exposed cells. (D) The effects of 60 minutes of ELF-EMF exposure on the steady-state inactivation of I_{Na}. The voltage protocol is shown below the current record. (E) Steady-state inactivation curves of I_{Na} for control and ELF-EMF-exposed cells. The data are from 6 (control) and 5 cells (ELF-EMF-exposed) and are expressed as means ± S.E.M.
doi:10.1371/journal.pone.0054376.g002

for 10 min, 30 min, 60 min or 90 min, the PGE₂ content obtained from three independent experiments was significantly increased by 9.6% ±5.3%, 23.9% ±4.8%, 20.9% ±6.2% and 19.2% ±5.9%, respectively ($n = 3$, $P<0.05$). We also assessed the levels of intracellular AA, which can be metabolically converted to PGE₂, using a direct rat AA ELISA kit to address whether the increase in PGE₂ after ELF-EMF exposure was the result of an increase in intracellular AA. The results in Fig. 6B showed that the intracellular AA levels were significantly increased following exposure to ELF-EMF. When cerebellar GCs were exposed to ELF-EMF for 10 min, 30 min, 60 min or 90 min, the intracellular AA levels measured in three independent experiments were significantly increased by 9.25±5.45%, 25.21±1.26%, 43.8±1.23% and 17.64±7.4%, respectively ($n = 4$, $P<0.05$).

AA is converted to prostaglandins by either the cyclooxygenase, the lipoxygenase or the monooxygenase pathways [27]. In particular, cyclooxygenase-2 (COX-2) is reported to play a key role in the release of PGE₂ [28]. To test that the increase in I_{Na} after ELF-EMF exposure was due to an increase in intracellular AA, we investigated the effect of the selective COX-2 inhibitors flufenamaic acid (FA) and niflumic acid (NA). Administration of 10 μM FA or 20 μM NA alone reduced the I_{Na} amplitude of cerebellar GCs by 23.6% ±1.2% ($n = 4$) and 14.7% ±2.3% ($n = 8$), respectively. In the presence of 10 μM FA or 20 μM NA, the increase in I_{Na} induced by ELF-EMF exposure was abolished (Fig. 6C and 6D). The I_{Na} density in cerebellar GCs

exposed to ELF-EMF for 60 min was increased by only 14.3±3.4% ($n = 8$) or 6.3±2.7% ($n = 10$), respectively, which were significantly different from those derived from cerebellar GCs exposed to ELF-EMF alone (125.6% ±8.26%, $n = 16$). Similarly, FA or NA treatment abolished the increase in PGE₂ release induced by ELF-EMF exposure (Fig. 6E). Data obtained from three independent experiments showed that the release of PGE₂ from cerebellar GCs exposed to ELF-EMF for 60 min was only increased by 3.3% ±3.0% and 2.6±1.5% in the presence of FA or NA, respectively.

To ascertain the role of COX in mediating the effects of ELF-EMF on cerebellar GCs, we determined the activities of both COX-1 and COX-2 using selective COX-1 and COX-2 ELISA kits. When cerebellar GCs were exposed to ELF-EMF for lengths of time ranging from 10 min to 90 min, the intracellular activity of COX-1 was increased from 5.0±1.2% to 6.3±2.2% (Fig. 7A) while the activity of COX-2 was increased from 6.1±2.6% to 9.7±3.9% (Fig. 7B). Hence, neither COX-1 nor COX-2 activity was significantly different than non-ELF-EMF-exposed cells. These data suggest that the increase in PGE₂ release after exposure to ELF-EMF was due to an increase in intracellular AA rather than in COX enzyme activity.

Given that cytosolic phospholipase A₂ (cPLA₂) also plays an important role in producing intracellular AA [29], we measured the activity of intracellular cPLA₂ in cerebellar GCs before and after ELF-EMF exposure using an ELISA kit and immunocytochemistry. As shown in Fig. 7C, ELF-EMF exposure significantly
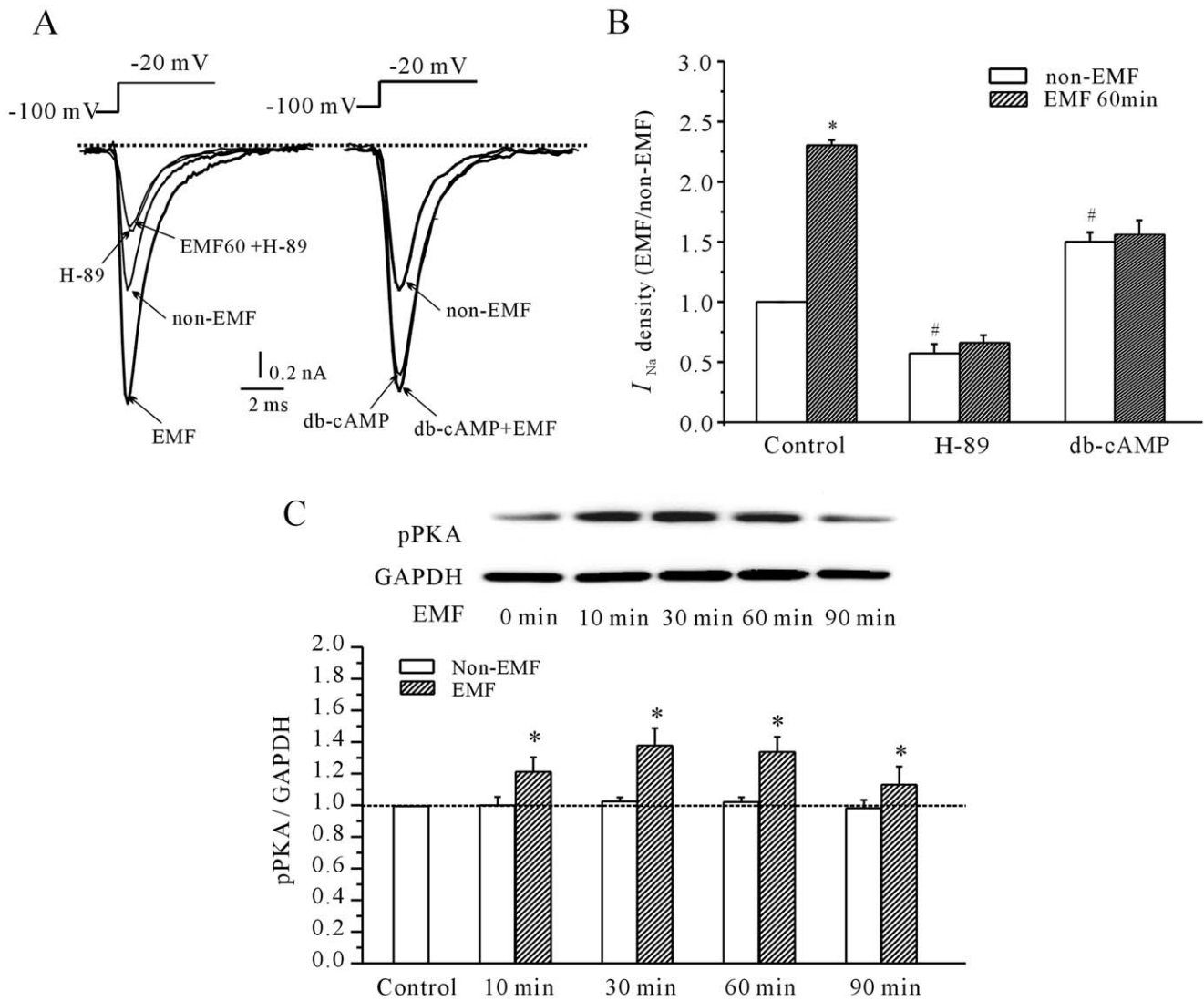
Figure 3. Involvement of the PKA pathway in the increase in I_{Na} induced by ELF-EMF exposure. (A) Current traces show the inhibitory effects of the selective PKA antagonist H-89 and db-cAMP on the increase in I_{Na} induced by a 60-minute exposure to a 1 mT ELF-EMF. (B) Statistical analysis of the inhibitory effects of H-89 and db-cAMP on the increase in I_{Na} density induced by a 60-minute exposure to a 1 mT ELF-EMF. The data are reported as the mean $\pm$ S.E.M. from 10–12 cells. *, $P<0.05$ compared to control (non-ELF-EMF group) using a Student's t-test. #, $P<0.05$ compared to the corresponding control (without H-89 and db-cAMP) non-ELF-EMF group using a Student's t-test. (C) Western blot analysis of the effects of ELF-EMF exposure on cellular pPKA levels. Upper panels show representative samples; the statistical analysis is shown in the lower panels; *, $P < 0.05$ compared to the corresponding control using Student's t-test.
doi:10.1371/journal.pone.0054376.g003

enhanced cPLA$_2$ activity, especially in the first 10 min to 30 min after exposure. Data obtained from four independent experiments indicated that exposing cerebellar GCs to ELF-EMF for 10 min, 30 min, 60 min or 90 min significantly increased cPLA$_2$ activity by 19.78±6.93%, 15.25±2.7%, 5.92±1.61% and 1.76±2.0%, respectively ($n = 4$, $P<0.05$). The effects of ELF-EMF exposure on intracellular cPLA$_2$ levels in cerebellar GCs were confirmed by immunostaining. As shown in Fig. 7D, a low level of cPLA$_2$ labeling was detected in cerebellar GCs without exposure to ELF-EMF (Fig. 7D, left). After exposure to ELF-EMF, cerebellar GCs showed a significant increase in staining for cPLA2 (Fig. 7D, right), indicating that ELF-EMF exposure significantly increased intracellular cPLA$_2$ levels. A model depicting the possible mechanisms involved in the modulation of I_{Na} by ELF-EMF exposure in cerebellar GCs is shown in Fig. 8.

Discussion

Although ELF-EMF exposure has been previously reported to modulate the activity of ion channels, few studies to date have measured the effects of EMF exposure on neuronal I_{Na}. Here, we report for the first time that ELF-EMF exposure enhances I_{Na} in cerebellar GCs. In particular, exposure of cerebellar GCs to ELF-EMF influences the activity of PLA$_2$, thus stimulating the production of intracellular AA, which is then converted to PGE$_2$. PGE$_2$ then enters the extracellular space and binds to EP receptors, activating the cAMP/PKA pathway and accounts for the induction of I_{Na}.
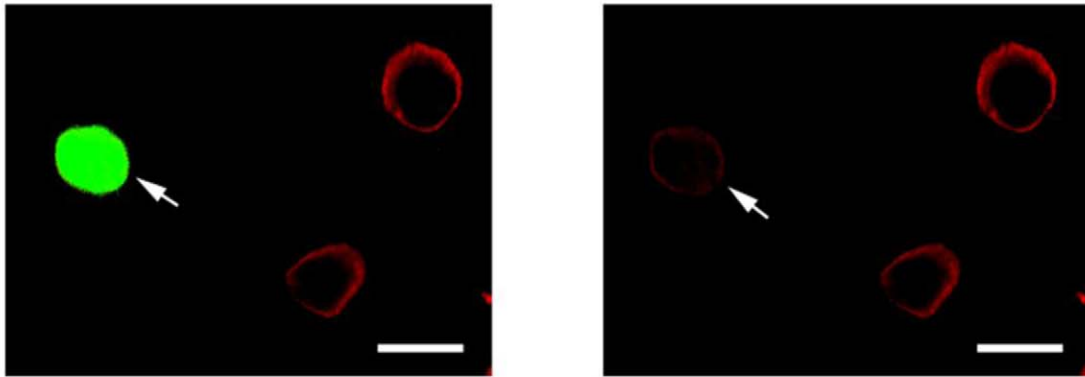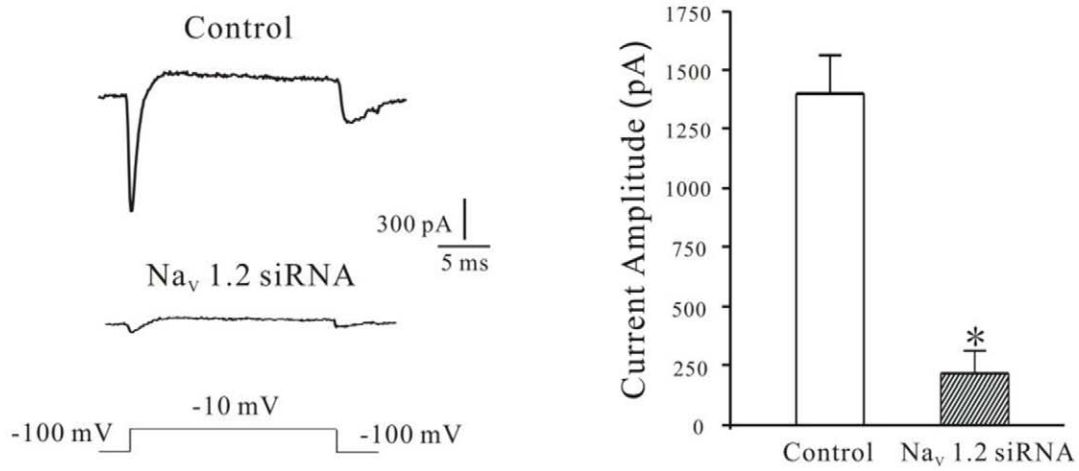
Figure 4. ELF-EMF exposure increased the Na$_V$1.2 α-subunit on the membrane in cerebellar GCs. (A) Cells expressing Na$_V$ 1.2 were labeled with Na$_V$1.2 specific antibody (red one) and transfected GC cells showing strong eGFP expression (left, see arrowhead). Cells transfected with siRNA vectors (same cell in the right, see arrowhead) showed dramatic reduction in Na$_V$ 1.2 expression. Scale bar was 10 μM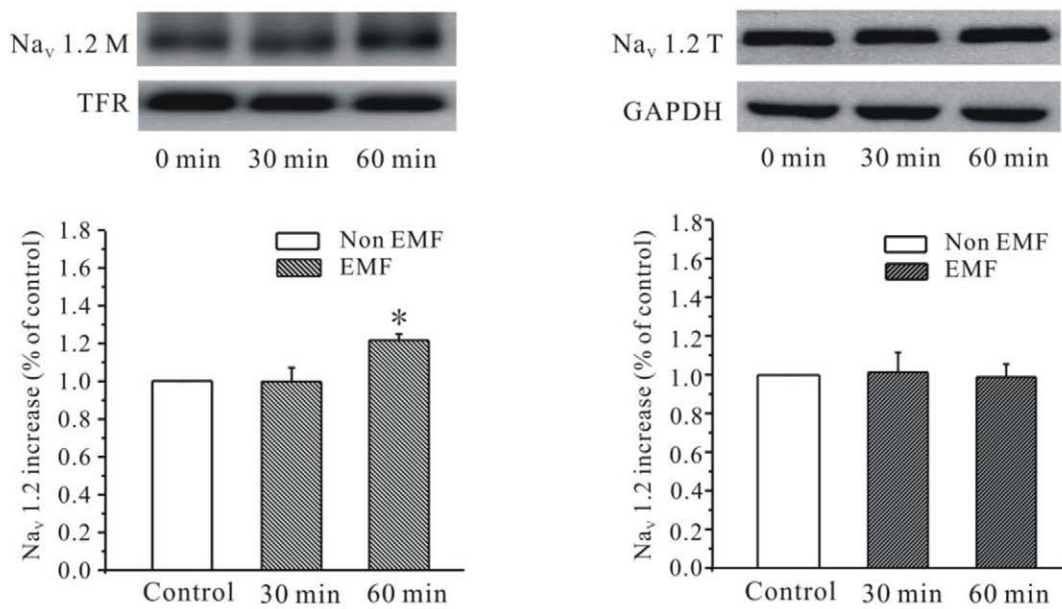. (B) The current recordings in a control cell and a post-transfected cell of Na$_V$ 1.2 siRNA plus eGFP. Current evoked by a 20 ms depolarizing pulse from a holding potential of −100 to −20 mV. (C) Na$_V$ 1.2 protein on membrane surface (Na$_V$ 1.2 M) was detected with the biotinylation assay after 30 or 60-minute exposure to a 1 mT ELF-EMF. Upper panels show representative samples, TFR (transferrin) was used as the loading control; the statistical analysis is shown in the lower panels. *, $P< 0.05$ compared to the corresponding control using Student's t-test. (D) Western blot analysis of the total level of Na$_V$ 1.2 expression (Na$_V$ 1.2 T) after 30 or 60-minute exposure to a 1 mT ELF-EMF.
doi:10.1371/journal.pone.0054376.g004

ELF-EMF Increases I$_{Na}$ in Rat Cerebellar GCs and Alters Na$_V$ Channel Kinetics

Although several ion channels, such as Ca^{2+} and Ca^{2+}-activated K$^+$ channels [8,9], are known to be modulated by EMF, the effects of EMF on Na$_V$ channels are poorly understood. Arthur D. Rosen's studies in GH3 cells indicated that there was a slight shift in the current-voltage relationship and a less than 5% reduction in peak current during 125 mT static magnetic field exposure [30].The authors speculated that a physical deformation in the liquid crystal membrane may be associated with these changes [30]. However, the changes observed in the steady-state activation characteristics of Na$_V$ channel kinetics during exposure to ELF-EMF in our study are due to an AA metabolite-induced increase in I$_{Na}$, a result that is similar to those obtained previously [22]. Interestingly, the effects of ELF-EMF on carbonic anhydrase entrapped in liposomes seem to exclude the role of protein molecules but in favor of a direct action on charged lipids of the membrane [7]. Moreover, in experiments using Ca^{2+}-activated K$^+$ channels in dorsal root ganglion-isolated neurons, Marchionni

et al. did not observe modifications in single-channel behavior that suggested a direct action of EMF on membrane proteins [8], consistent with the hypothesis that ELF-EMF-stimulated enhancement of I$_{Na}$ in rat cerebellar GCs is not related directly to physical changes within the membrane and that an AA metabolism-related pathway might be involved. The discrepancy of these two reports may be due to the use of different cell type and different form of EMF source.

The time course for the effects of ELF-EMF on the activity of Na$_V$ in this study is noteworthy. In previous studies, the effects of exposure to EMF differed significantly based on whether the exposure occurred for minutes, hours or days. Here, we demonstrate that exposure to ELF-EMF induced similar effects on I$_{Na}$ in rat cerebellar GCs regardless the condition is 1 mT stimulation for a short time or 0.4 mT stimulation for a longer time. Notably, it is generally believed that short-term changes induced by EMF are mediated by modifications in enzyme activity in the cytosol or the membrane [4,31,32] while the long-term exposure to EMF may induce changes in nuclear functions such as gene transcription and cell cycle regulation [33,34]. Moreover, a
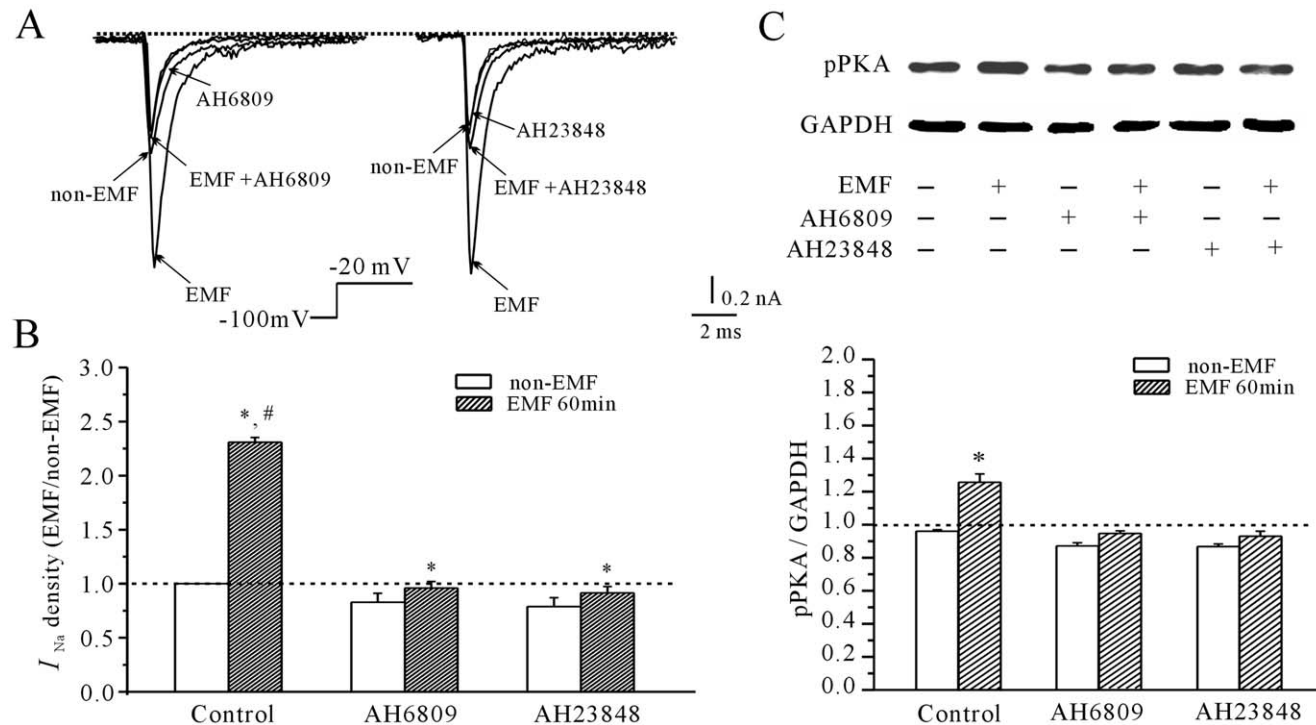
Figure 5. Effects of EP receptor antagonists on the increase in I$_{Na}$ density induced by ELF-EMF exposure. (A) Current traces show the blocking effect of the EP2 and EP4 receptor antagonists AH6809 and AH23848 on the increase in I$_{Na}$ induced by a 60-minute exposure to a 1 mT ELF-EMF. (B) Statistical analysis of the inhibitory effect of AH6809 and AH23848 on the I$_{Na}$ density increase induced by a 60-minute exposure to a 1 mT ELF-EMF. #, $P<0.05$ compared to the corresponding control (non-ELF-EMF) using Student's t-test. *, $P<0.05$ compared to ELF-EMF exposure alone using a Student's t-test. (C) Western blot analysis of the inhibitory effect of AH6809 and AH23848 on intracellular PKA phosphorylation induced by a 60-minute exposure to a 1 mT ELF-EMF. Upper panels show representative samples; the statistical analysis is shown in the lower panels; *, $P< 0.05$ compared to the corresponding control using Student's t-test.
doi:10.1371/journal.pone.0054376.g005
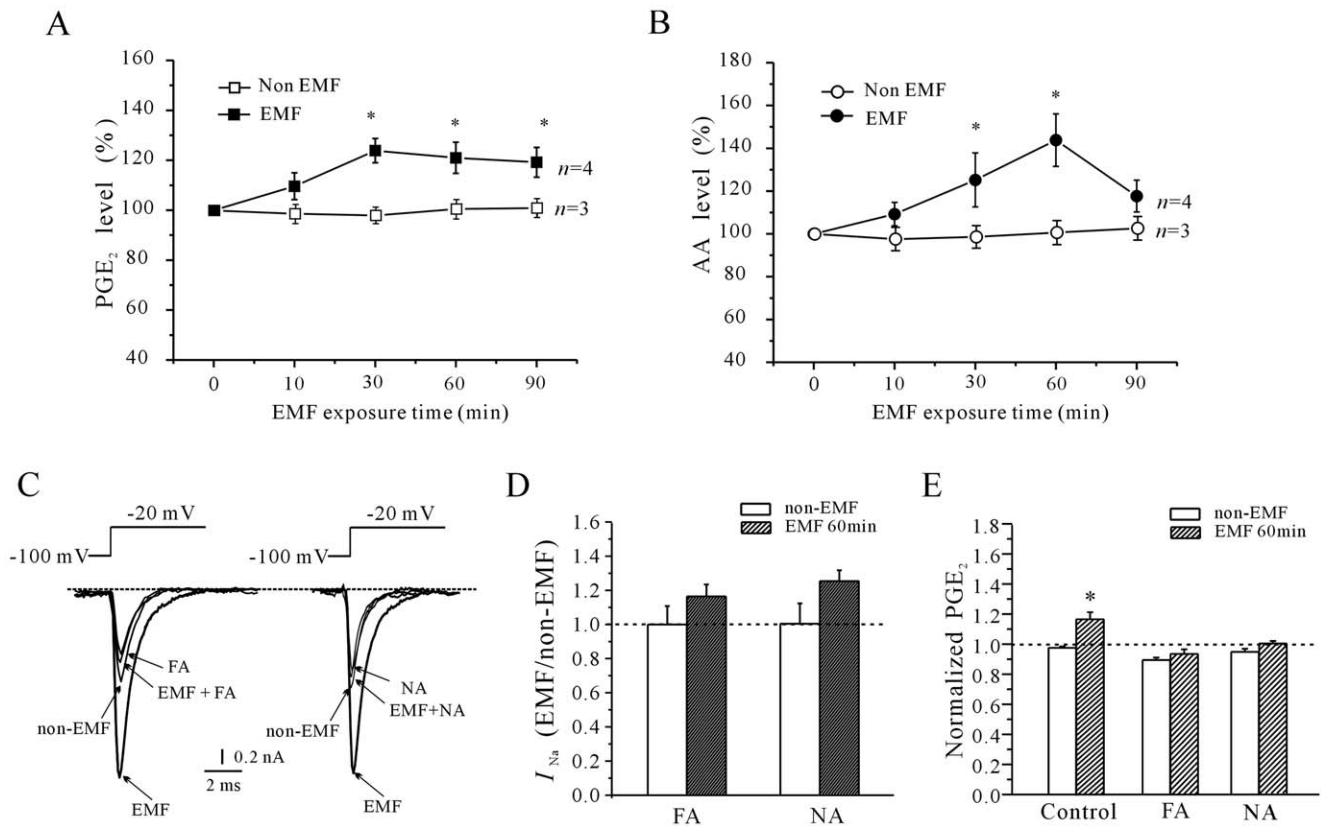
Figure 6. Effects of the AA/PGE$_2$ pathway on the ELF-EMF exposure-induced increase in I_{Na} in cerebellar GCs. (A) PGE$_2$ release from cerebellar GCs exposed to 1 mT ELF-EMF for various lengths of time. The data are from three and four independent experiments, respectively. *, $P<$ 0.05 compared to the corresponding control using Student's t-test. (B) Intracellular AA levels in cerebellar GCs exposed to 1 mT ELF-EMF for various lengths of time. The data are from three and four independent experiments, respectively. *, $P<$ 0.05 compared to the corresponding control using Student's t-test. (C) Current traces show the inhibitory effects of the COX-2 inhibitors flufenamaic acid (FA) and niflumic acid (NA) on the increase in I_{Na} induced by 60 minutes of exposure to a 1 mT ELF-EMF. (D) Statistical analysis of the effects of FA and NA on the increase in I_{Na} induced by a 60-minute exposure to a 1 mT ELF-EMF. (E) Statistical analysis of the effects of FA and NA on PGE$_2$ release induced by a 60-minute exposure to a 1 mT ELF-EMF.
doi:10.1371/journal.pone.0054376.g006

previous study in cerebellar GCs indicated that a five-day EMF exposure contributes to premature expression of GluRs, and leads to more rapid cellular maturation [35]. To avoid the influence of multiple factors due to long-term EMF exposure, we performed all our experiments at 1 mT EMF exposure for a short time, which we believe it is well-suited to access the effect of ELF-EMF on intracellular signaling pathways.

ELF-EMF Exposure Enhances I$_{Na}$ via PGE$_2$-mediated Activation of the cAMP/PKA Pathway

It has been reported that the cAMP/PKA pathway can modulate Na$_V$ activity. In particular, the α-subunits of Na$_V$ channels are preferred substrates for phosphorylation by cAMP/ PKA [36]. Either activation or inhibition of Na$_V$ channels has been reported, which is probably due to the difference in cell model used [37,38]. Our previous study demonstrated that intracellular application of AA increases the activity of Na$_V$ via the activation of the cAMP/PKA pathway in cerebellar GCs [22]. Consistent with the previous findings, we observed that the PKA signaling plays an important role in the increase in I_{Na} after exposure to ELF-EMF. In light of our findings that ELF-EMF activates PKA signaling (Fig. 3), modifies steady state properties of the Na$_V$ (Fig. 2) and increases insertion of Na$_V$ into the membrane (Fig. 4), we speculate that the effect of ELF-EMFs on I_{Na} is likely

exerted at multiple levels. In addition to the changes in voltage-gating property and insertion of additional Na$_V$ channels into the membrane, exposure to ELF-EMFs may also modulate the single channel properties by phosphorylation of channel protein. Recording of single-channel activity, however, is of technically challenging and requires specialized set up for such precise measurement. Nonetheless, the possible regulation of Na$_V$ channels upon PKA phosphorylation warrants future investigations.

Previous studies by Sibylle Thumm et al. reported that ELF-EMF (20 Hz, 7–8 mT) exposure for 60 min resulted in an increase in PKA activity in human skin fibroblasts and rat embryonic osteoblasts [39]. The underlying mechanism by which PKA was activated by ELF-EMF exposure, however, was not known. In synovial fibroblasts of an osteoarthritis patient, ELF-EMF exposure-induced changes in cAMP levels were associated with a selective increase in adenosine receptor expression [33]. Similarly, our results indicate that exposure to ELF-EMF induces an increase in PKA activity and that treatment with EP2 and EP4 antagonists abolished this effect. Moreover, we observed that, along with EP receptor activation, PGE$_2$ levels were also increased following ELF-EMF exposure. Our data indicate that the effects of ELF-EMF exposure on PKA activity might not reflect a direct effect on this enzyme. Rather, PKA activation is mediated by elevations of
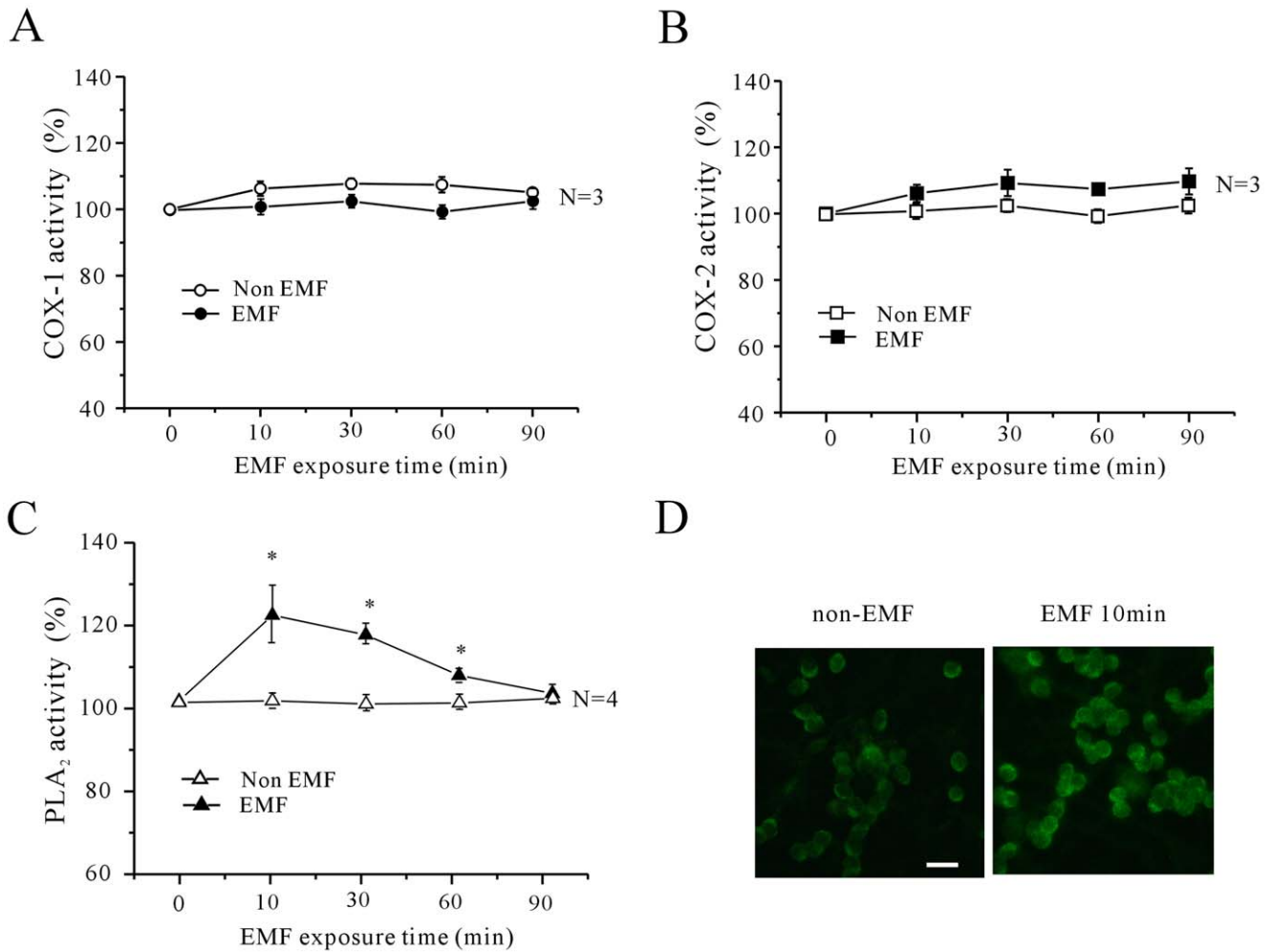
Figure 7. Effects of exposure to a 1 mT ELF-EMF on intracellular COX-1, COX-2 and cPLA$_2$ activities in cerebellar GCs. (A and B) COX-1 and COX-2 activity were measured in cerebellar GCs exposed to a 1 mT ELF-EMF for various lengths of time. The data are from three and four independent experiments, respectively. (C) cPLA$_2$ activity was measured in cerebellar GCs exposed to a 1 mT ELF-EMF for various lengths of time. *, $P < 0.05$ compared to the corresponding control using a Student's t-test. (D) Immunostaining showing the effects of ELF-EMF exposure on intracellular cPLA$_2$ levels. The scale bar represents 20 μm.
doi:10.1371/journal.pone.0054376.g007

PGE$_2$, which then binds to the EP receptors to modulate PKA activity.

Increases in Intracellular PLA$_2$ Activity and AA Levels are Critical Steps in the ELF-EMF-mediated Enhancement of I$_{Na}$

It is well known that intracellular PGE$_2$ is derived from AA via the cyclooxygenase (COX) pathway, which includes COX-1 and COX-2 [28], and COX-2 has been reported to be the most abundant COX isozyme in neurons [40]. In our study, intracellular PGE$_2$ and AA levels were increased in cerebellar GCs following ELF-EMF exposure. Neither COX-1 nor COX-2 activity was significantly enhanced by ELF-EMF exposure. Inhibiting COX activity with specific inhibitors, however, eliminated the ELF-EMF exposure-induced increase in I_{Na}. Hence, an alternative pathway is likely involved for the increase in intracellular PGE$_2$ levels after ELF-EMF exposure.

In brain tissue, AA is mainly released downstream of cPLA$_2$. In this study, our results showed that intracellular AA levels in cerebellar GCs were significantly increased after EMF exposure.

cPLA$_2$ activity, which is important for rapid AA release in neurons, was also significantly enhanced by exposure to ELF-EMF, suggesting that the increases in cPLA2 activity and AA levels are critical steps in the ELF-EMF-induced enhancement of I_{Na}. Using a cell-free PLA$_2$ assay, Song et al. failed to observe changes in PLA$_2$, including cPLA$_2$ and sPLA$_2$, following exposure to ELF-EMF (60 Hz, 0.1 or 1 mT) for 4 or 6 h [41]. The difference in these findings compared to our results in cerebellar GCs could be due to the use of a cell-free PLA$_2$ assay as cell membranes play an important role in mediating the effects of EMF on enzymatic activity [31]. Despite there is evidence for the involvement of cPLA2 activity in the responses to a wide variety of stimuli such as oxidative stress and inflammatory factors [42,43], the relevant mechanism of ELF-EMF exposure-induced cPLA$_2$ activation remains unclear.

Physiological Implications

The effects of ELF-EMF on nerve cells have been extensively studied in various organisms [8,35]. Although the reported results are variable or contradictory due to differences in the experimental conditions and in the density and/or duration of EMF
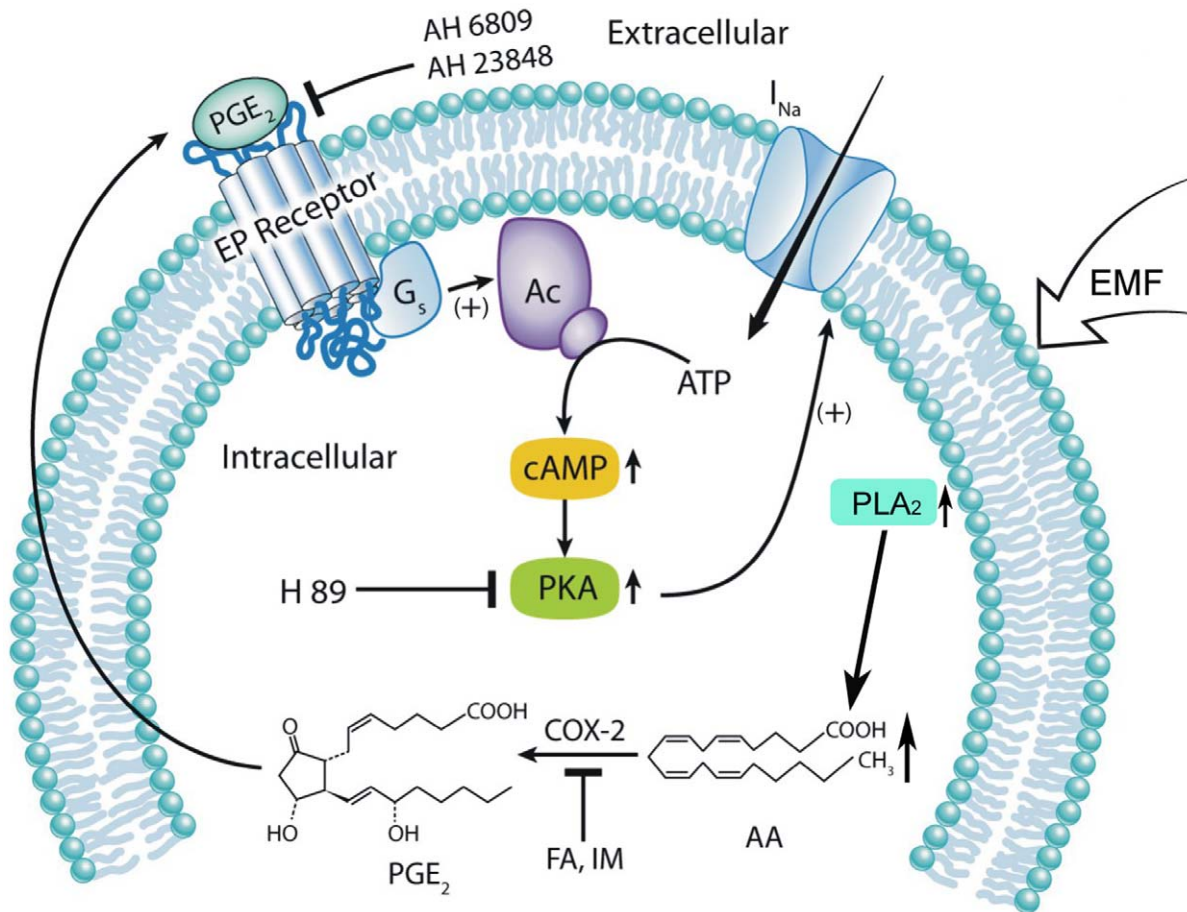
Figure 8. A proposed model depicting the mechanisms that are likely to be involved in the modulation of I_{Na} by ELF-EMF exposure in cerebellar GCs. ELF-EMF active cPLA$_2$ and up-regulated AA and PGE2, which can act in an autocrine or paracrine manner to activate EP receptors. Ligand binding of EP2/4 is associated with PKA activation and consequently modulates I_{Na}. (+), activation; (−), inhibition.
doi:10.1371/journal.pone.0054376.g008

exposure, EMF has recently been reported to modulate of neuronal excitatory functions and neurogenesis [8,14,15]. In addition, recent studies have revealed an important role for cPLA2 in the modulation of neuronal excitatory functions [29]. The findings from our molecular-level analysis of the macroscopic effects on I_{Na} produced by exposure to ELF-EMF provide evidence for an important effect of EMF on neuronal excitation in the CNS. We also observed that the effects of ELF-EMF exposure on cerebellar GCs peaked and then declined with extended exposure time. Notably, this phenomenon was observed for I_{Na} and also for enzyme activities. The observed effects is likely due to the cells reach equilibrium through self-regulation after the initial ELF-EMF exposure and its effect on cPLA$_2$ and I_{Na}. Nonetheless, the modulatory effects on neuronal excitatory caused by exposure to ELF-EMF are complicated and varied. Therefore, further exploration is required to comprehensively analyze the physiological and/or pathological effects of ELF-EMF exposure on I_{Na}, along with the resulting neuronal consequences.

Materials and Methods

Ethics Statement

This study was carried out in strict accordance with the recommendations in the Guide for the Care and Use of Laboratory Animals of the National Institutes of Health. The protocol was approved by the Committee on the Ethics of Animal Experiments of the Fudan University (Permit Number: 20090614-001). All surgery was performed under sodium pentobarbital anesthesia, and all efforts were made to minimize suffering.

Primary Cell Culture

Cells were derived from cerebellum of 7-day-old Sprague–Dawley rat pups as described previously [44]. Isolated cells were then plated onto 35-mm-diameter Petri dishes coated with poly-L-lysine (1 µg/ml) at a density of $2.5 \times 10^5/cm^2$. Cultured cells were incubated at 37°C with 5% CO$_2$ in Dulbecco's Modified Eagle's Medium (DMEM) supplemented with 10% fetal calf serum, glutamine (5 mM), insulin (5 µg/ml), KCl (25 mM), and 1% antibiotic–antimycotic solution. All experiments were carried out with cerebellar GCs during 6–8 days in culture (DIC).

Electromagnetic Field Production

The system used to expose cerebellar GCs cells to electromagnetic fields was the same used in previous studies, with some revisions (I-ONE, Shanghai, China) [33,45,46]. Briefly, a 50 Hz magnetic field was generated by a pair of Helmholtz coils placed in opposition to each other. The coils were powered by a generator system that produced the input voltage of the pulse, and the magnetic flux densities could be regulated within the range of 0 to 1.0 mT. The device was powered by an AC power generator, and

the EMF frequency and density were monitored by an EMF sensor that was connected to a digital multimeter. The geometry of the system assured a uniform field for the exposed cultured cells. The surfaces of the culture plates were parallel to the force lines of the alternating magnetic field in the solenoid. Air and culture medium temperatures were continuously monitored for the duration of experiments. The maximum temperature increase recorded in the cultures that were exposed to ELF-EMF (compared to non-exposed cultures) was $0.4\pm0.1°C$. To identify any possible influence of this increase on our results, we compared data obtained from cerebellar GCs cultured in two different CO_2 incubators at temperature settings of 37.0 and 37.4°C, and the results is consistent. The incubator was keep closed all throughout the EMF or non-EMF experiments to make sure that the conditions stable. Non-EMF groups were incubated in the same incubator in which the conditions were the same as for the exposed groups but without EMF.

Patch-clamp Recordings

Whole-cell currents of granule neurons were recorded using a conventional patch-clamp technique. In 6–8 DIC cerebellar granule cells, transient I_{Na} are largely unclamped because of an event generated at a site electrotonically distant from the soma and prone to escape from clamp control, presumably the axon [47]. Therefore, we choose those cells that relatively isolated and only record currents without unclamped spike. Prior to current recordings, the culture medium was replaced with a bath solution containing (in mM): NaCl 145, KCl 2.5, HEPES 10, MgCl$_2$ 1 and glucose 10 (pH adjusted to 7.4 using NaOH). Soft glass recording pipettes were filled with an internal solution containing (in mM): CsCl 145, HEPES 10, MgCl$_2$ 2, and EGTA 5 (pH adjusted to 7.3 using CsOH). The pipette resistance was 5–6 MΩ after filling with the internal solution. Whole cell series resistances of 6–8 MΩ were routinely compensated by more than 70%. All recordings were performed at room temperature (23–25C°).

Intracellular AA Assay

Intracellular AA levels in cerebellar GCs were measured as previously described [48], with minor modifications. Briefly, 1×10^5 cells were plated in 35-mm dishes and grown to confluence. The cells were washed with 1 mL of bath solution and cerebellar GCs were exposed to 1 mT ELF-EMF for 10 min, 30 min, 60 min or 90 min. The media was then removed, and 0.3 mL of 0.45% NP40 (Sigma, St. Louis, MO, USA) was added to the plates. After a 5-minute incubation on ice, the lysate was removed from the plates and centrifuged for 5 minutes at 4°C. The supernatant was collected and assayed for AA levels using a direct rat AA ELISA kit (R&B, Yueyan Bio-Tech, Shanghai, China) according to the manufacturer's instructions. The data represent the means of several experiments, as indicated in the figure legends.

PGE$_2$ Release Assay

PGE$_2$ levels in the culture media were measured using highly sensitive enzyme-linked immunosorbent assay kits (R&B, Yueyan Bio-Tech, Shanghai, China) according to the manufacturer's instructions. Briefly, 1×10^5 cells were plated in 35-mm dishes and grown to confluence. The cells were washed with 1 mL of bath solution and were exposed to a 50 Hz, 1 mT EMF for 10 min, 30 min, 60 min or 90 min. The media were then collected and centrifuged for 5 minutes at 4°C. The supernatant was collected and assayed for levels of PGE$_2$. The data represent the means of several experiments, as indicated in the figure legends.

COX-1, COX-2 and PLA$_2$ Enzyme Activity Assays

COX-1, COX-2 and PLA$_2$ activities in cerebellar GCs were measured using highly sensitive, enzyme-linked immunosorbent assay kits (R&B, Yueyan Bio-Tech, Shanghai, China) according to the manufacturer's instructions. Briefly, 1×10^5 cells were plated in 35-mm dishes and grown to confluence. The cells were washed with 1 mL of bath solution and were exposed to 1 mT ELF-EMF for 10 min, 30 min, 60 min or 90 min. The media was then removed, and the cells were diluted with PBS (pH 7.2–7.4) until the cell concentration reached 1 million cells/ml. Following repeated freeze-thaw cycles, which result in cell damage and the release of intracellular components, the supernatant was collected by centrifugation for 20 min at 2000–3000 rpm and assayed for COX-1, COX-2 and PLA$_2$ activities. The data represent the means of several experiments, as indicated in the figure legends.

Phosphorylated Protein Kinase A Assay

The cells were lysed in HEPES-NP40 lysis buffer (20 mM HEPES, 150 mM NaCl, 0.5% NP-40, 10% glycerol, 2 mM EDTA, 100 μM Na$_3$VO$_4$, 50 mM NaF, pH 7.5, and 1% proteinase inhibitor cocktail) on ice for 30 min. After centrifugation, the supernatant was mixed with 2× sodium dodecyl sulfate loading buffer and boiled for 5 min. The proteins were separated on a 10% polyacrylamide gel, transferred to polyvinylidene difluoride membranes (Millipore, MA, USA), blocked with 10% nonfat milk and incubated at 4°C overnight with a rabbit polyclonal antibody against the phosphorylated form of the PKA catalytic subunits (1:1000; Santa Cruz Biotechnology Inc., CA, USA) or a rabbit monoclonal antibody against GAPDH (1:1000; Sigma). After extensive washing with TBST, the membrane was incubated with horseradish peroxidase-conjugated anti-mouse or anti-rabbit IgG (1:10,000) (KangChen Bio-Tech, China) for 2 h at room temperature. Chemiluminescent signals were generated using a SuperSignal West Pico trial kit (Pierce, USA) and detected using a ChemiDoc XRS System (Bio-Rad Laboratories, Inc., CA, USA). The protein measurements were normalized to GAPDH and control/GAPDH as 1.0.

Biotinylation Assay

Cell surface proteins were biotinylated according to the product instruction and previously described [49]. Briefly, the neurons were incubated with 0.25 mg/mL of Sulfo-NHS-SS-biotin (Thermo scientific, Rockford, USA) for 45 min at 4°C, and then the reaction is blocked with 50 mM Tris (pH 8.0) for 20 min at 4°C. Cells were lysed in HEPES-NP40 lysis buffer. Biotinylated proteins were pulled down with Streptavidin Agrose Beads (Thermo scientific, Rockford, USA) overnight at 4°C and washed for 4 times with lysis buffer. The bound proteins were eluted by the sample buffer and analyzed by western blotting.

Immunocytochemistry

To detect changes in cPLA$_2$ in cerebellar GCs following exposure to ELF-EMF, an immunocytochemical assay was performed using the following procedure. Isolated cortical neurons plated on coverslips were washed three times with 0.01 M PBS and then fixed with 4% PFA for 30 minutes, rinsed three times with PBS and pre-incubated for 1 hour in 6% normal donkey serum (v/v) in PBS plus 0.1% Triton X-100 at room temperature. The cells were then incubated with a rabbit anti-cPLA$_2$ antibody (1:100 dilution, Santa Cruz Biotechnology Inc., CA, USA) for 2 hours in a humidified air chamber. After incubation, the cells were rinsed three times with PBS and then further incubated with a secondary donkey anti-rabbit IgG tagged with FITC (1:100

dilution, Jackson ImmunoResearch Laboratories, West Grove, PA) for 30 minutes at room temperature. The coverslips were then rinsed twice in PBS and mounted onto glass slides. For labeling of the Na_v 1.2 subunit, specific mouse monoclonal antibodies (from UC Davis/NINDS/NIMH NeuroMab Facility) were used as the primary antibody (at a working dilution of 1: 200). TRITC conjugated goat anti-mouse immunoglobulin G (1: 200 dilution, from Jackson Immunoresearch Laboratories, West Grove, PA) was used as the secondary antibody.

siRNA design

Gene specific siRNA duplexes were designed to be homologous to $Na_{V1.2}$ mRNA consensus sequence (GenBank accession number X03639). Primers for loop and 3′P-dT extensions contained 19-nt siRNA were commercially obtained (Invitrogen). The sense strand of the siRNA (5′-GGATATTGGTTCCGAAAAT-3′), homologous to nt 1965–1983 of the Na_V mRNA sequence, was chosen according to the recommendations by others (http://www.dharmacon.com/DesignCenter/DesignCenterPage.aspx). Restriction site Sac I was added to the 3′ tail of resulting molecule to facilitate ligating to LentiLox 3.7.

Data Acquisition and Analysis

All currents were recorded using an Axopatch 200 B amplifier (Axon Instruments, Foster City, CA, USA) that was operated in voltage-clamp mode. A Pentium computer was connected to the recording equipment with a Digidata 1300 analog-to-digital (A/D) interface. The current was digitally sampled at 100 μs (10 kHz), and the current signals were filtered using a 5-kHz, five-pole Bessel filter. The currents were corrected online for leak and residual capacitance transients using a P/4 protocol. Data acquisition and analysis were performed using pClamp 8.01 software (Axon Instruments, Foster City, CA, USA) and/or Origin6.1 (MicroCal, Northampton, MA, USA). Statistical analysis was performed using Student's t-test with non-paired or paired comparisons as relevant. The values are given as the means $\pm$ S.E.M., with n representing the number of cells tested. A value of $P<0.05$ was considered a significant statistical difference between groups. When multiple comparisons were made, the data were analyzed by a one-way ANOVA.

Chemicals

All drugs used were purchased from Sigma-Aldrich (St. Louis, MO, USA) except for the fetal calf serum. The DMEM culture medium and antibiotic–antimycotic solution were obtained from Gibco Life Technologies (Grand Island, NY, USA). The arachidonic acid, 5,8,11,14-eicosatetraynoic acid, flufenamic acid, phorbol-12-myristate-13-acetate, AH6809 and AH23848 were first dissolved in DMSO and then diluted in extracellular solution to a final DMSO concentration of <0.2%, which by itself, did not affect I_{Na}.

Author Contributions

Conceived and designed the experiments: YAM YLH. Performed the experiments: YLH DDL YJF XQZ. Analyzed the data: YLH DDL JJY. Contributed reagents/materials/analysis tools: YJF XQZ JJY. Wrote the paper: YAM YLH.

References

1. Cui Y, Ge Z, Rizak JD, Zhai C, Zhou Z, et al. (2012) Deficits in water maze performance and oxidative stress in the hippocampus and striatum induced by extremely low frequency magnetic field exposure. PLoS One 7: e32196.
2. Luukkonen J, Liimatainen A, Hoyto A, Juutilainen J, Naarala J (2011) Pre-exposure to 50 Hz magnetic fields modifies menadione-induced genotoxic effects in human SH-SY5Y neuroblastoma cells. PLoS One 6: e18021.
3. Piacentini R, Ripoli C, Mezzogori D, Azzena GB, Grassi C (2008) Extremely low-frequency electromagnetic fields promote in vitro neurogenesis via upregulation of Ca(v)1-channel activity. J Cell Physiol 215: 129–139.
4. Arendash GW, Mori T, Dorsey M, Gonzalez R, Tajiri N, et al. (2012) Electromagnetic treatment to old Alzheimer's mice reverses beta-amyloid deposition, modifies cerebral blood flow, and provides selected cognitive benefit. PLoS One 7: e35751.
5. Dibirdik I, Kristupaitis D, Kurosaki T, Tuel-Ahlgren L, Chu A, et al. (1998) Stimulation of Src family protein-tyrosine kinases as a proximal and mandatory step for SYK kinase-dependent phospholipase Cgamma2 activation in lymphoma B cells exposed to low energy electromagnetic fields. J Biol Chem 273: 4035–4039.
6. Sun WJ, Chiang H, Fu YT, Yu YN, Xie HY, et al. (2001) Exposure to 50 Hz electromagnetic fields induces the phosphorylation and activity of stress-activated protein kinase in cultured cells. Electromagnetic Biology and Medicine 20: 415–423.
7. Ramundo-Orlando A, Mattia F, Palombo A, D'Inzeo G (2000) Effect of low frequency, low amplitude magnetic fields on the permeability of cationic liposomes entrapping carbonic anhydrase: II. No evidence for surface enzyme involvement. Bioelectromagnetics 21: 499–507.
8. Marchionni I, Paffi A, Pellegrino M, Liberti M, Apollonio F, et al. (2006) Comparison between low-level 50 Hz and 900 MHz electromagnetic stimulation on single channel ionic currents and on firing frequency in dorsal root ganglion isolated neurons. Biochim Biophys Acta 1758: 597–605.
9. Grassi C, D'Ascenzo M, Torsello A, Martinotti G, Wolf F, et al. (2004). Effects of 50 Hz electromagnetic fields on voltage-gated Ca²⁺ channels and their role in modulation of neuroendocrine cell proliferation and death. Cell Calcium 35: 307–315.
10. Waxman SG (2007) Channel, neuronal and clinical function in sodium channelopathies: from genotype to phenotype. Nat Neurosci 10: 405–409.
11. Banasiak KJ, Burenkova O, Haddad GG (2004) Activation of voltage-sensitive sodium channels during oxygen deprivation leads to apoptotic neuronal death. Neuroscience 126: 31–44.
12. Ding Y, Brackenbury WJ, Onganer PU, Montano X, Porter LM, et al. (2008) Epidermal growth factor upregulates motility of Mat-LyLu rat prostate cancer cells partially via voltage-gated Na⁺ channel activity. J Cell Physiol 215: 77–81.
13. Fraser SP, Diss JK, Chioni AM, Mycielska ME, Pan H, et al. (2005) Voltage-gated sodium channel expression and potentiation of human breast cancer metastasis. Clin Cancer Res 11: 5381–5389.
14. Aldinucci C, Carretta A, Maiorca SM, Leoncini S, Signorini C, et al. (2009) Effects of 50 Hz electromagnetic fields on rat cortical synaptosomes. Toxicol Ind Health 25: 249–252.
15. Cuccurazzu B, Leone L, Podda MV, Piacentini R, Riccardi E, et al. (2011) Exposure to extremely low-frequency (50 Hz) electromagnetic fields enhances adult hippocampal neurogenesis in C57BL/6 mice. Exp Neurol 226: 173–182.
16. Liu Z, Fei XW, Fang YJ, Shi WJ, Zhang YQ, et al. (2008) PLC-dependent intracellular Ca²⁺ release was associated with C6-ceramide-induced inhibition of Na+ current in rat granule cells. J Neurochem 106: 2463–2475.
17. Schaller KL, Caldwell JH (2003) Expression and distribution of voltage-gated sodium channels in the cerebellum. Cerebellum 2: 2–9.
18. D'Mello SR, Galli C, Ciotti T, Calissano P (1993) Induction of apoptosis in cerebellar granule neurons by low potassium: inhibition of death by insulin-like growth factor I and cAMP. Proc Natl Acad Sci U S A 90: 10989–10993.
19. Jiao S, Liu Z, Ren WH, Ding Y, Zhang YQ, et al. (2007) cAMP/protein kinase A signalling pathway protects against neuronal apoptosis and is associated with modulation of Kv2.1 in cerebellar granule cells. J Neurochem 100: 979–991.
20. Hu CL, Zeng XM, Zhou MH., Shi YT, Cao H, et al. (2008) Kv 1.1 is associated with neuronal apoptosis and modulated by protein kinase C in the rat cerebellar granule cell. J Neurochem 106: 1125–1137.
21. Liu Z, Fei XW, Fang YJ, Shi WJ, Zhang YQ, et al. (2008) PLC-dependent intracellular Ca²⁺ release was associated with C6-ceramide-induced inhibition of Na+ current in rat granule cells. J Neurochem 106: 2463–2475.
22. Fang YJ, Zhou MH, Gao XF, Gu H, Mei YA (2011) Arachidonic acid modulates Na+ currents by non-metabolic and metabolic pathways in rat cerebellar granule cells. Biochem J 438: 203–215.
23. Catterall WA, Goldin AL, Waxman SG (2005) Nomenclature and structure-function relationships of voltage-gated sodium channels. Pharmacol Rev 57: 397–409.
24. Narumiya S, Sugimoto Y, Ushikubi F (1999) Prostanoid receptors: structures, properties, and functions. Physiol Rev 79: 1193–1226.
25. Zahner G, Schaper M, Panzer U, Kluger M, Stahl RA, et al. (2009) Prostaglandin EP2 and EP4 receptors modulate expression of the chemokine CCL2 (MCP-1) in response to LPS-induced renal glomerular inflammation. Biochem J 422: 563–570.
26. Fulton AM, Ma X, Kundu N (2006) Targeting prostaglandin E EP receptors to inhibit metastasis. Cancer Res 66: 9794–9797.
27. Brash AR (2001) Arachidonic acid as a bioactive molecule. J Clin Invest 107: 1339–1345.

28. Zeldin DC (2001) Epoxygenase pathways of arachidonic acid metabolism. J Biol Chem 276: 36059–36062.

29. Sun GY, Xu J, Jensen MD and Simonyi A (2004) Phospholipase A2 in the central nervous system: implications for neurodegenerative diseases. J Lipid Res 45: 205–213.

30. Rosen AD (2003) Effect of a 125 mT static magnetic field on the kinetics of voltage activated Na$^+$ channels in GH3 cells. Bioelectromagnetics 24: 517–523.

31. Morelli A, Ravera S, Panfoli I, Pepe IM (2005) Effects of extremely low frequency electromagnetic fields on membrane-associated enzymes. Arch Biochem Biophys 441: 191–198.

32. Ravera S, Bianco B, Cugnoli C, Panfoli I, Calzia D, et al. (2010) Sinusoidal ELF magnetic fields affect acetylcholinesterase activity in cerebellum synaptosomal membranes. Bioelectromagnetics 31: 270–276.

33. Ongaro A, Varani K, Masieri FF, Pellati A, Massari L, et al. (2011) Electromagnetic fields (EMFs) and adenosine receptors modulate prostaglandin E(2) and cytokine release in human osteoarthritic synovial fibroblasts. J Cell Physiol 227: 2461–2469.

34. Richard D, Lange S, Viergutz T, Kriehuber R, Weiss DG, et al. (2002) Influence of 50 Hz electromagnetic fields in combination with a tumour promoting phorbol ester on protein kinase C and cell cycle in human cells. Mol Cell Biochem 232: 133–141.

35. Lisi A, Ciotti MT, Ledda M, Pieri M, Zona C, et al. (2005) Exposure to 50 Hz electromagnetic radiation promote early maturation and differentiation in newborn rat cerebellar granule neurons. J Cell Physiol 204: 532–538.

36. England S, Bevan S, Docherty RJ (1996) PGE$_2$ modulates the tetrodotoxin-resistant sodium current in neonatal rat dorsal root ganglion neurones via the cyclic AMP-protein kinase A cascade. J Physiol 495 (Pt 2): 429–440.

37. Gold MS, Levine JD, Correa AM (1998) Modulation of TTX-R I_{Na} by PKC and PKA and their role in PGE2-induced sensitization of rat sensory neurons in vitro. J Neurosci 18: 10345–10355.

38. Costa MR and Catterall WA (1984) Cyclic AMP-dependent phosphorylation of the alpha subunit of the sodium channel in synaptic nerve ending particles. J Biol Chem 259: 8210–8218.

39. Thumm S, Loschinger M, Glock S, Hammerle H, Rodemann HP (1999) Induction of cAMP-dependent protein kinase A activity in human skin fibroblasts and rat osteoblasts by extremely low-frequency electromagnetic fields. Radiat Environ Biophys 38: 195–199.

40. Smith WL, Dewitt DL (1996) Prostaglandin endoperoxide H synthases-1 and -2. Adv Immunol 62: 167–215.

41. Song HS, Kim HR, Ko MS, Jeong JM, Kim YH, et al. (2010) Effect of Extremely Low Frequency Electromagnetic Fields (EMF) on Phospholipase Activity in the Cultured Cells. Korean J Physiol Pharmacol 14: 427–433.

42. Leslie CC (1997) Properties and regulation of cytosolic phospholipase A2. J Biol Chem 272: 16709–16712.

43. Gijon MA, Spencer DM, Siddiqi AR, Bonventre JV, Leslie CC (2000) Cytosolic phospholipase A2 is required for macrophage arachidonic acid release by agonists that Do and Do not mobilize calcium. Novel role of mitogen-activated protein kinase pathways in cytosolic phospholipase A2 regulation. J Biol Chem 275: 20146–20156.

44. Gonzalez B, Leroux P, Lamacz M, Bodenant C, Balazs R, et al. (1992) Somatostatin receptors are expressed by immature cerebellar granule cells: evidence for a direct inhibitory effect of somatostatin on neuroblast activity. Proc Natl Acad Sci U S A 89: 9627–9631.

45. De Mattei M, Varani K, Masieri FF, Pellati A, Ongaro A, et al. (2009) Adenosine analogs and electromagnetic fields inhibit prostaglandin E2 release in bovine synovial fibroblasts. Osteoarthritis Cartilage 17: 252–262.

46. Varani K, Vincenzi F, Targa M, Corciulo C, Fini M, et al. (2010) Effect of pulsed electromagnetic field exposure on adenosine receptors in rat brain. Bioelectromagnetics.

47. Diwakar S, Magistretti J, Goldfarb M, Naldi G, D'Angelo E (2009) Axonal Na+ channels ensure fast spike activation and back-propagation in cerebellar granule cells. J Neurophysiol 101: 519–532.

48. Reynolds JD, Brien JF (1992) Ontogeny of glutamate and gamma-aminobutyric acid release in the hippocampus of the guinea pig. J Dev Physiol 18: 243–252.

49. Yao H, Zhou K, Yan D, Li M, Wang Y (2009). The Kv2.1 channels mediate neuronal apoptosis induced by excitotoxicity. J Neurochem 108: 909–919.